Electronic Supplementary Material (ESI) for ChemComm.

Near-Field Engineering for Boosting the Photoelectrochemical Activity to a Modal Strong Coupling Structure

Yanfeng Cao,[a] Xu Shi,[b] Tomoya Oshikiri,[a] Shuai Zu,[a] Yuji Sunaba,[a] Keiji Sasaki[a] and Hiroaki Misawa[*a,c]*

[a]Research Institute for Electronic Science, Hokkaido University, Sapporo, Japan.

[b]Creative Research Institution, Hokkaido University, Sapporo, Japan.

[c]Center for Emergent Functional Matter Science, National Chiao Tung University, Hsinchu, Taiwan.

Corresponding Author

* E-mail: misawa@es.hokudai.ac.jp.

Experimental section

Sample Preparation. Silica glass substrates (10 × 10 × 1.0 mm^3) were ultrasonically cleaned for 5 min each in acetone, methanol and deionized water. Then, the substrates were dried with a pure nitrogen flow. A 100 nm Au film and a 2-nm titanium film were sputtered in sequence on the surface of the silica glass using a Helicon sputtering system (ULVAC, MPS-4000C1/HC1). Afterward, a 28 nm titanium dioxide (TiO_2) thin film was deposited onto the Au film using a commercial hot-wall flow-type atomic layer deposition (ALD) reactor (SUNALETM R series (Picosun)) with titanium tetrachloride ($TiCl_4$) and H_2O as precursors; the deposition temperature was held at 300 ºC. A 3-nm Au thin film was sequentially evaporated in a thermal evaporator at a deposition rate of 0.1 Å•s^{-1}. Finally, the samples were annealed in air at 300 °C for 2 h, and the Au-NPs appeared on the TiO_2 film surface. To fabricate the partially inlaid Au NPs, a 7-nm TiO_2 thin film was additionally deposited on by ALD. Then, the samples were annealed in air at 300 °C for 2 h.

Au was electrochemically postdeposited on ATA using a three-electrode system, with the ATA structure as the working electrode (WE), a platinum wire as the counter electrode (CE) and a saturated calomel electrode (SCE) as the reference electrode (RE). For the preparation of the WE, an In-Ga alloy (4:1 weight ratio) film was pasted onto the back and side of the structure, which was then connected to an electrochemical analyser (ALS/CH Instruments Model 852C) with a copper lead wire. The 0.25 mmol•dm^{-3} $HAuCl_4$ with 0.1 mol•dm^{-3} Na_2SO_4 was used as the Au precursor, in which Na_2SO_4 worked as a stabilizer and electrolyte. A +0.3 V bias was applied during the electrochemical deposition. The electrochemical reaction was performed for 1, 3 and 8

min. Finally, the as-prepared structure was rinsed with deionized water and dried with a pure nitrogen flow.

Numerical simulations. Full-field electromagnetic wave simulations were performed by using the finite-element method (FEM) (COMSOL Multiphysics®) for the Au-NP/TiO_2/Au-film (ATA) structure and Au@Au-NP/TiO_2/Au-film (Au@ATA) structure. The refractive index of gold was based on the data from Johnson and Christy.[1] The TiO_2 thin film was assumed to behave as a dielectric with an effective refractive index of n = 2.4. The background was water with the refractive index of n = 1.33. A unit cell of investigated structures was simulated using periodic boundary conditions in x- and y-directions and perfectly matched layers in z-direction. Circularly polarized plane waves with the wavelength of 650 nm were used to excite the structure along the z direction. The finest mesh size was 0.2 nm. An ellipsoid sphere with a diameter of 12 nm in the x and y directions and 10 nm in the z direction was used to model the Au-NP. The size of post-deposited Au was1.3 times of Au-NP. The period was 20 nm. The Au-NP/TiO_2 interface was formed by truncating Au NPs by TiO_2.

Characterization. The reflection and transmission spectra were obtained by a photonic multichannel analyzer (PMA-11 (Hamamatsu Photonics)) equipped with an optical microscope (BX-51 (Olympus)). The numerical aperture of the objective lens used for the measurements was 0.3. The surface morphology was observed by ultra-high-resolution scanning electron microscope (SU8230 (HITACHI)) with a maximum resolution of 0.8 nm at an electron accelerating voltage of 15 kV. The cross-section was analyzed by high-resolution transmission electron microscopy (JEOL ARM (200 F) 200 kV FEG-STEM/TEM) with a resolution of 75 pm at an electron accelerating voltage of 200 kV.

Photoelectrochemical measurements. The typical current-potential curves were achieved using a three-electrode system, with the obtained structure as the working electrode (WE), a platinum wire as the counter electrode (CE) and a saturated calomel electrode (SCE) as the reference electrode (RE). For the preparation of the WE, an In- Ga alloy (4 :1 weight ratio) film was pasted onto the back of the structure, which was then connected to an electrochemical analyser (ALS/CH Instruments Model 852C) with a copper lead wire. The 0.1 mol•dm^{-3} KOH aqueous solution was used as the supporting electrolyte solution without any specific electron donor. An 800 W xenon lamp was used as the light source. For the IPCE calculation, the photocurrent was measured at +0.3 V vs. SCE. The IPCE was calculated by the following equation:

$$IPCE(\lambda) = \frac{1240 \text{ x } I\ (A/cm^2)}{\lambda(nm) \text{ x } P\ (W/cm^2)}$$

where I was the photocurrent density generated by monochromatic light with a bandwidth of less than 15 nm, λ is the wavelength of the monochromatic incident light, and P is the light intensity.

Supplementary Data

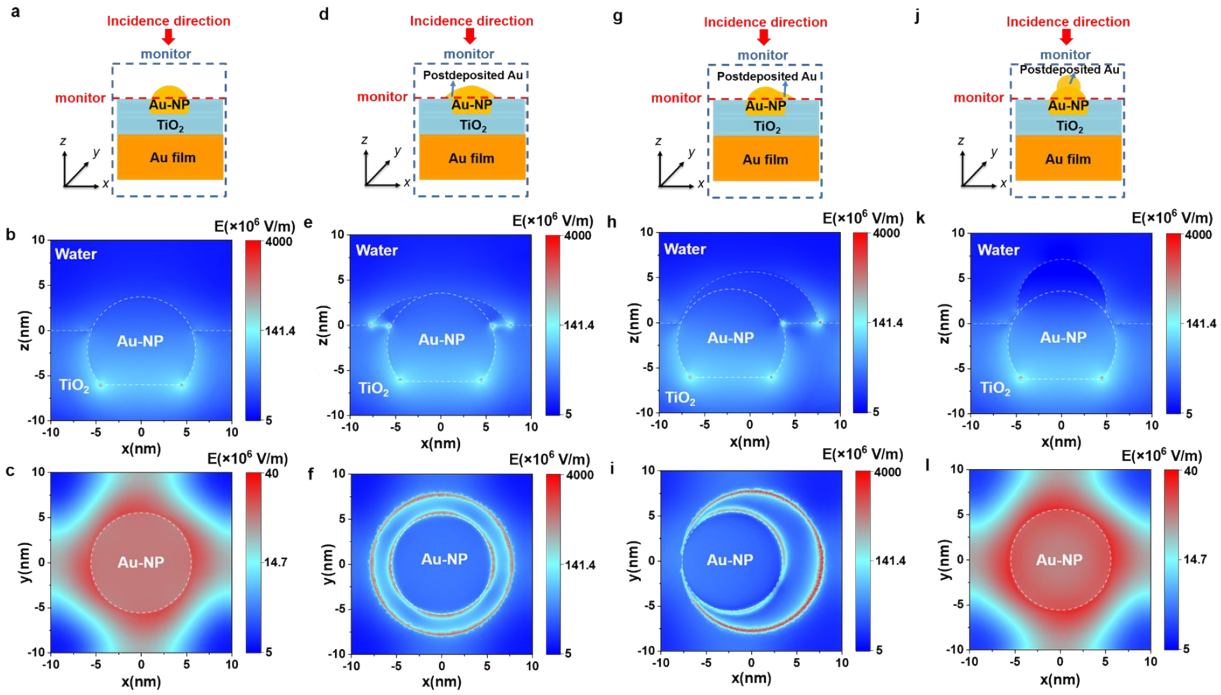

Figure S1. Near-field distribution under 650 nm irradiation calculated using an FEM simulation. Two near-field profile monitors were set in the *xz*- and *xy*-planes to visualize the near-field intensity, as shown by the blue and red dashed lines. (a) Simulation model, (b) side view (*xz*-plane), obtained by magnifying part of (a), (c) top view (*xy*-plane) of ATA structures; (d) simulation model, (e) side view (*xz*-plane), obtained by magnifying part of (d), (f) top view (*xy*-plane) of Au@ATA with the postdeposited Au locating around the original Au-NP; (g) simulation model, (h) side view (*xz*-plane), obtained by magnifying part of (g), (i) top view (*xy*-plane) of Au@ATA with the postdeposited Au locating at one side of the original Au-NP; (j) simulation model, (k) side view (*xz*-plane), obtained by magnifying part of (j), (l) top view (*xy*-plane) of Au@ATA with the postdeposited Au locating at the top of the original Au-NP; The simulations were performed with a circularly polarized plane-wave light source in water.

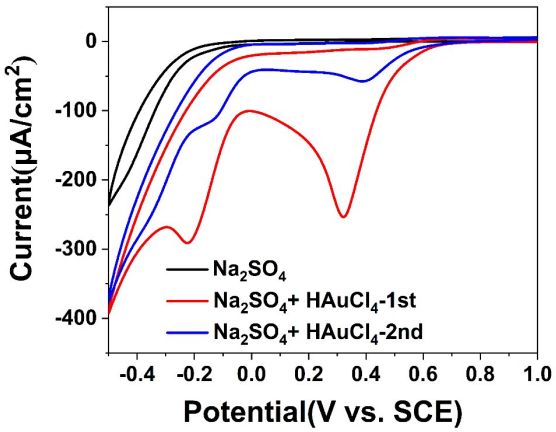

Figure S2. Cyclic voltammogram (CV) curves recorded on ATA electrode in 0.1 mol•dm^{-3} Na_2SO_4 solution containing 0.25 mmol•dm^{-3} $HAuCl_4$, red and blue line are first and second scan, respectively; black line is CV recorded under the same conditions in the absence of $HAuCl_4$. Scan direction: from positive potential to negative potential. Scan rate: 0.01 mV•s^{-1}.

In order to determine the deposition potential of mushroom-like Au on ATA electrode in 0.1 mol•dm^{-3} Na_2SO_4 solution containing 0.25 mmol•dm^{-3} $HAuCl_4$, the cyclic voltammogram (CV) curves with the range of scanned potentials from 1.0 V to -0.5 V were obtained using the as-prepared pure ATA structure as the working electrode, Pt wire as the counter electrode, and SCE as the reference electrode. As previously reported in the literature, Na_2SO_4 was used as supporting electrolyte in order to avoid aggregation. On the first positive potential to negative potential forward scan (red line), the reduction peaks displayed at 0.32 V vs SCE, which were absent when recording CV in $HAuCl_4$ free Na_2SO_4 solution, is recognized as the reduction of Au^{3+} on ATA electrode. It is related to the well-known three-electron reduction process of Au^{3+} which leads to the formation of metallic Au on the electrode surface.[2] The relevant equation can be expressed as Equation. (1):

$$\mathbf{AuCl_4^- + 3e^- \rightarrow Au + 4Cl^-} \quad \mathbf{E^\circ = 1.00\ V/SHE} \qquad (1)$$

However, on the second positive potential to negative potential forward scan (blue line), this peak was shifted about +0.1 V vs SCE to higher potential, in line with thermodynamics which predicts an easier growth of previously formed Au than nucleation of new Au on ATA structures. It should be noted that this phenomenon was not accompanied by a current crossover on the first backward scan, contrary to what has been described in many reports. This phenomenon could be explained by the fact that the relatively low difference of energy required for the nucleation of Au on ATA and on Au (as shown by the little potential shift of Au^{3+} reduction peak between first and second forward scans, respectively) and the very cathodic inversion potential (−0.5 V) which induced an important contribution of the diffusion according to Cottrell's law(current proportional to $t^{-1/2}$). As reported, high over-potential was deemed to increase nucleation rate by increasing the free energy for formation of new nuclei.[2] Therefore, applied potential in the electrodeposition procedure could significantly influence the surface morphology of the structure. Thus, the electrodeposition potential is fixed at +0.3 V vs. SCE in the present work.

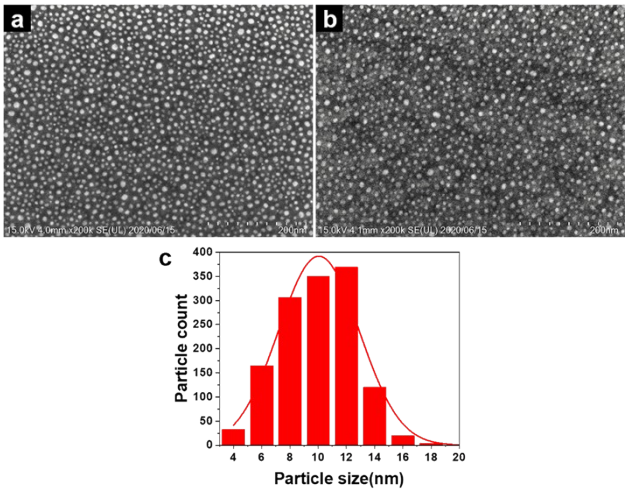

Figure S3. Morphology and size distribution of Au-NPs. (a) SEM image of Au-NPs/TiO_2/Au-film without inlaid. (b) SEM image of Au-NPs/TiO_2/Au-film with 7 nm inlaid depth. The scale bar is 200 nm. (c) Size distribution of the Au-NPs by analysing (a). The red line shows the Gaussian fitting. The Au-NP size was found to be 10 nm ± 6.7 nm.

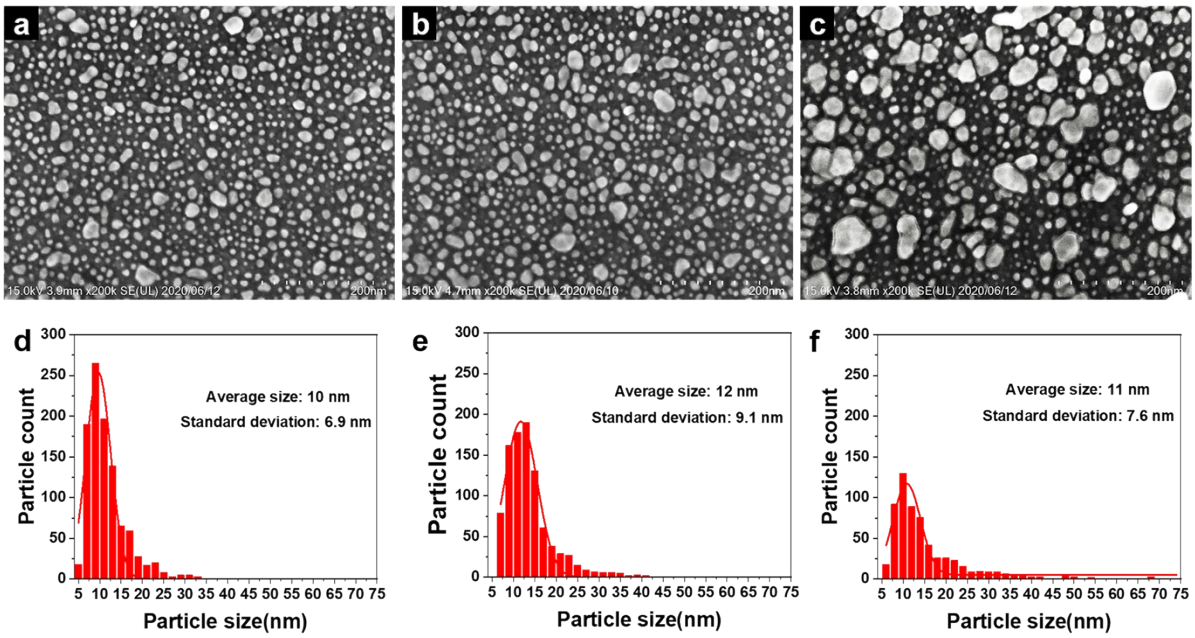

Figure S4. Surface morphologies of Au@ATA with different electrochemical deposition time. (a), (b), (c) The respective top view SEM images for 1 min, 3 min, 8 min. (d), (e), (f) The respective Au-NPs size distribution analyzed from the corresponding SEM images. The scale bar is 200 nm.

The area of selected SEM images is 639 nm × 479 nm (Figure S3a, S4a, S4b and S4c). There are 1367 Au-NPs for ATA (Figure S3a) in the selected SEM image and 1023, 951, 618 Au-NPs for Au@ATA with the electrochemical deposition time of 1 min, 3 min and 8 min (Figure S4a, S4b and S4c).

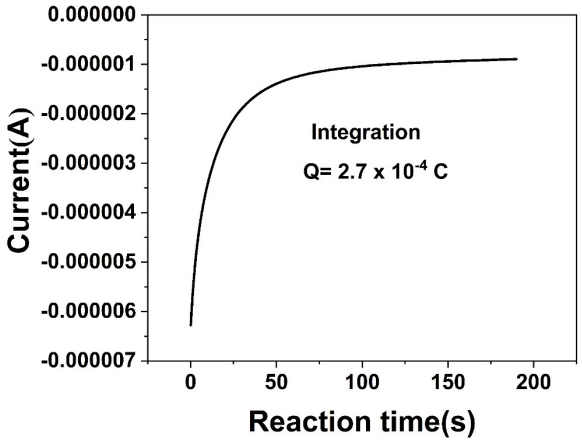

Figure S5. The current–time curve recorded on ATA working electrode in 0.1 mol•dm^{-3} Na_2SO_4 solution containing 0.25 mmol•dm^{-3} $HAuCl_4$, a platinum wire and a SCE were employed as the counter electrode and reference electrode, respectively. The working electrode potential was set to + 0.3 V versus (vs) SCE.

During the electrochemical postdepositing process, the current-time curve recorded on ATA working electrode in 0.1 mol•dm^{-3} Na_2SO_4 solution containing 0.25 mmol•dm^{-3} $HAuCl_4$ was illustrated in Figure S5. After 3 min electrochemical reaction, the overall charge was integrated as 2.7x10^{-4} C. Therefore, 1.40×10^{14} Au atoms were post-deposited on Au-NPs/TiO_2/Au-film structure. On the other hand, by analysing the SEM images of Au@ATA with 3 min electrochemical deposition, there were about 1.15×10^{14} Au atoms postdeposited on ATA structure. Therefore, the Faradic efficiency for 3 min deposition was 82.4 %.

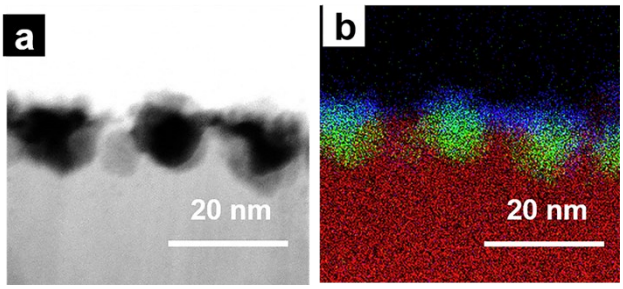

Figure S6. Electrochemically postdeposited Pt on ATA structures. (a) STEM image and (b) EDX of ATA with electrochemically postdeposited Pt (Pt@ATA). Pt was electrodeposited in presence of 0.25 mmol•dm^{-3} H_2PtCl_6 (Chloroplatinic acid hexahydrate) with 0.1 mol•dm^{-3} Na_2SO_4 aqueous solution with an applied potential -0.1 V vs SCE for 3 min. The red, green and blue colours depict TiO_2, Au, Pt, respectively.

In line with the parameters of postdeposited Au, platinum (Pt) was electrodeposited on ATA structures with an applied potential of -0.1 vs. SCE. Figure S6 showed the STEM image and EDX of ATA structure with postdeposited Pt, from which it was clear to see that large amounts of monodispersed ultrasmall Pt were uniformly and intimately deposited on the ATA framework. The corresponding energy-dispersive X-ray spectroscopy mapping was given in Figure S6b and clearly showed that the mushroom-like Pt nanoparticles was uniformly deposited on the ATA structure.

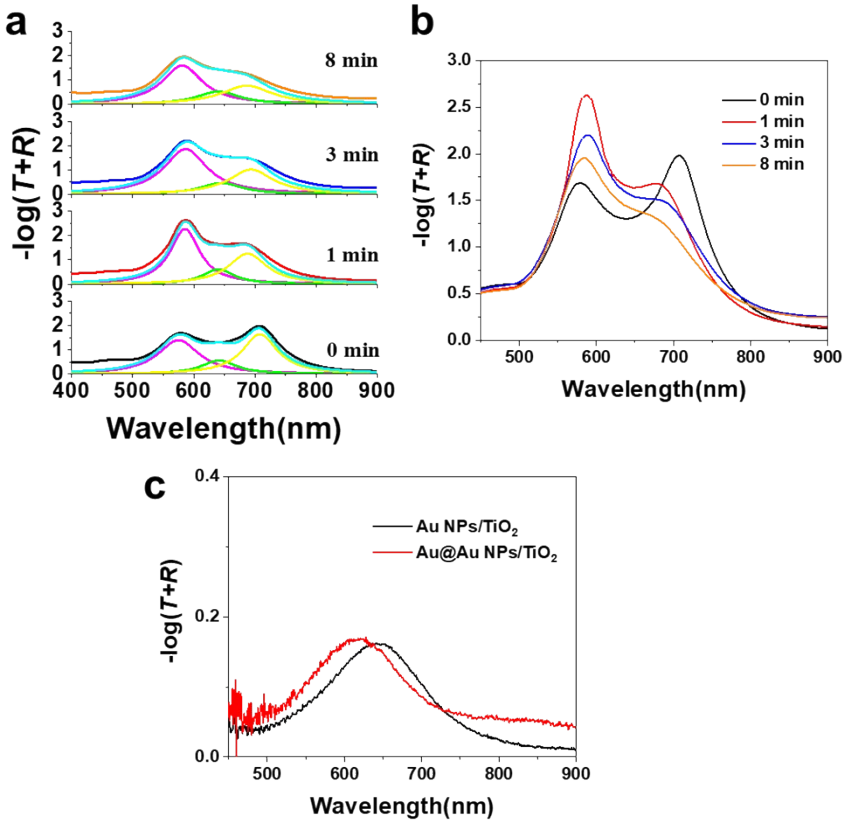

Figure S7. (a, b) Absorption spectra of the Au@ATA structures with varying electrochemical postdeposition times. The thickness of TiO_2 was 28 nm. The superimposed curved in magenta, green and yellow indicate the fitting of three peaks and the cyan curves are sum of them in panel (a). (c) Absorption spectra of the Au-NPs on TiO_2 before (black) and after (red) postdepositing Au.

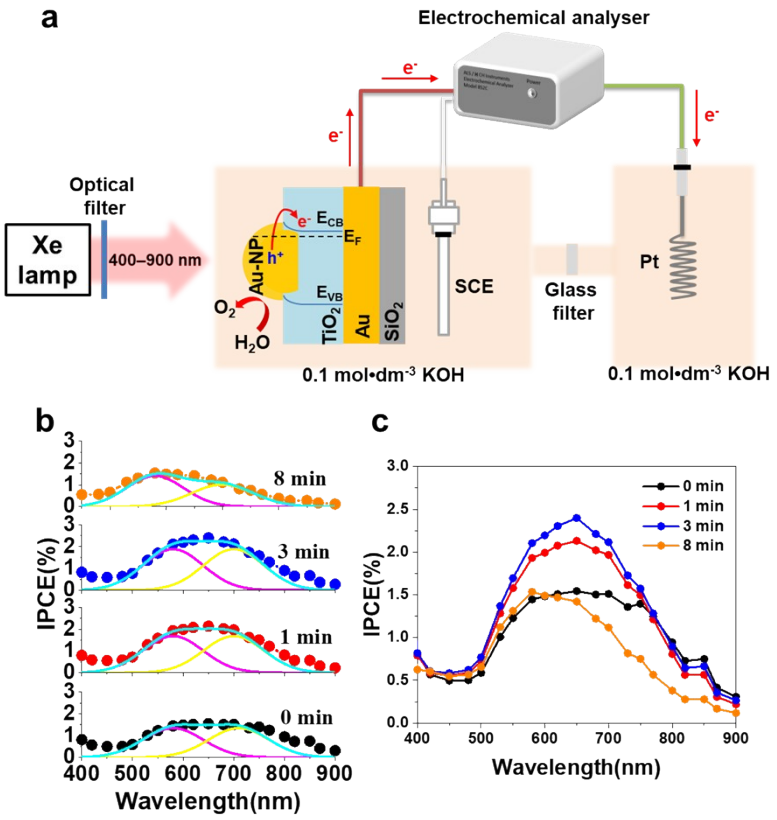

Figure S8. (a) Schematic of the three-electrode system used for the photoelectrochemical measurements. E_{CB} and E_{VB} refer to conduction band and valence band energy of TiO_2. E_F is the Femi level of Au and TiO_2. (b, c) IPCE action spectra of Au@ATA photoelectrodes with different deposition times. The superimposed curved in magenta and yellow indicate the fitting of two peaks and the cyan curves are sum of them in panel (b).

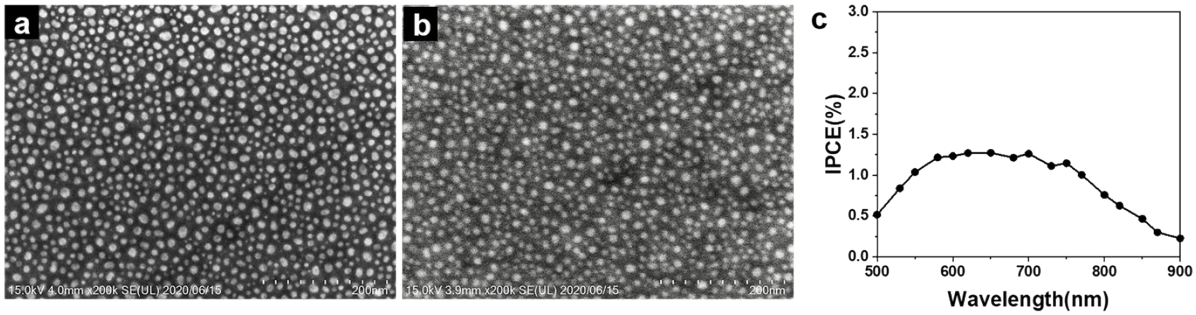

Figure S9. ATA with 20 nm Au-NP size and an inlaid depth of 7 nm. SEM images before (a) and after (b) 7 nm inlaid, (c) IPCE action spectrum of the corresponding structure.

References

1 P. B. Johnson and R. W. Christy, *Phys. Rev. B*, 1972, **6**, 4370.

2 G. Gotti, K. Fajerwerg, D. Evrard and P. Gros, *Electrochim. Acta*, 2014, **128**, 412–419.